

Metal contacts to n-GaN

L. Dobos^{a,*}, B. Pécz^a, L. Tóth^a, Zs.J. Horváth^a, Z.E. Horváth^a,
A. Tóth^a, E. Horváth^a, B. Beaumont^b, Z. Bougrioua^c

^a *Research Institute for Technical Physics and Materials Science, Hungarian Academy of Sciences, H-1525, Budapest, P.O. Box 49, Hungary*

^b *LUMILOG, 2720, Chemin Saint Bernard, Les Moulins 1, F-06220 Vallauris, France*

^c *CRHEA, CNRS, Rue B. Grégory, Sophia-Antipolis, F-06560 Valbonne, France*

Received 11 November 2005; received in revised form 23 December 2005; accepted 23 December 2005

Available online 13 February 2006

Abstract

Al, Au, Ti/Al and Ti/Au contacts were prepared on n-GaN and annealed up to 900 °C. The structure, phase and morphology were studied by cross-sectional transmission and scanning electron microscopy as well as by X-ray diffraction (XRD), the electrical behaviour by current–voltage measurements. It was obtained that annealing resulted in interdiffusion, lateral diffusion along the surface, alloying and bowling up of the metal layers. The current–voltage characteristics of as-deposited Al and Ti/Al contacts were linear, while the Au and Ti/Au contacts exhibited rectifying behaviour. Except the Ti/Au contact which became linear, the contacts degraded during heat treatment at 900 °C. The surface of Au and Ti/Au contacts annealed at 900 °C have shown fractal-like structures revealed by scanning electron microscopy. Transmission electron microscopy and XRD investigations of the Ti/Au contact revealed that Au diffused into the n-GaN layer at 900 °C. X-ray diffraction examinations showed, that new Ti₂N, Au₂Ga and Ga₃Ti₂ interface phases formed in Ti/Au contact at 900 °C, new Ti₂N phase formed in Ti/Al contact at 700 and 900 °C, as well as new AlN interface phase developed in Ti/Al contact at 900 °C.

© 2006 Elsevier B.V. All rights reserved.

PACS: 68.37.–d/68.37.Lp; 68.55.–a/68.55.Jk

Keywords: GaN; Thin films; Transmission electron microscopy; Solid phase reaction; Electrical properties

1. Introduction

GaN is a wide bandgap material (3.4 eV) and it is very promising for optoelectronic (LED's, lasers, detectors) and microelectronic (high-temperature, high-power and high-frequency transistors) applications due to its direct bandgap. The utilization of GaN-based devices is limited by several materials and engineering problems, including the difficulty in making low-resistance, thermally stable ohmic contacts, especially to n-type GaN. Although both Schottky and ohmic contacts to n-type GaN have been widely studied during the last decade, their properties and technologies are not yet cleared. One of the key questions for both types of contacts is the poor reproducibility of the results obtained in different laboratories for similar metallization. Another fundamental problem for

Schottky contacts is the occurrence of high reverse leakage currents [1,2]. For GaN and other highly ionic semiconductors the Schottky barrier heights of metal to III-nitride contacts strongly depend on the difference between the work function of the metal and the electron affinity of the semiconductor [3].

The progress of the semiconductor technology has aroused the requirement of new, highly reliable and cheap contact materials. The substitution of gold with aluminium should have numerous advantages. Hence the Al-based metallization offers a more homogeneous and sharper metal–semiconductor interface than the well-known Au-based ohmic metallization that is beneficial, for example, for the submicron-size devices.

Titanium-based metallization schemes have been used to form ohmic contacts to GaN [1,4–6]. During annealing solid phase reactions between Ti and GaN is possible [7]. Nitrogen out-diffuses from the GaN lattice to form TiN and residual nitrogen vacancies act as donors in GaN. The interfacial area thus becomes heavily doped providing the configuration needed for tunneling contacts [7].

* Corresponding author. Tel.: +36 1 392 2222; fax: +36 1 392 2273.

E-mail address: dobos@mfa.kfki.hu (L. Dobos).

In this work four different metallizations, namely Al, Au, Ti/Al and Ti/Au prepared to Si doped GaN layers and annealed at different temperatures have been studied by cross-sectional transmission electron microscopy (XTEM), selected area electron diffraction (SAED) and energy dispersive X-ray analysis (EDS), high resolution transmission electron microscopy (HREM), scanning electron microscopy (SEM), X-ray diffraction (XRD) analysis and by current–voltage (I – V) measurements.

2. Experimental

The GaN layer was grown on a c -plane sapphire substrate by MOCVD. First a 10.5 μm thick undoped GaN layer was grown using a process leading to a film with an ultra low dislocation density ($8 \times 10^7 \text{ cm}^{-2}$) [8], then a 4.7 μm thick Si doped layer was grown with a Hall free electron concentration of $2.5 \times 10^{18} \text{ cm}^{-3}$ and a sheet resistance of $20 \Omega/\text{sq}$.

Prior to metal deposition by thermal evaporation, the GaN-covered wafers were cleaned and etched in ultrasonically agitated acetone bath for 5 min and in dilute HF:H₂O (1:10) for 2 min and then they were 3 \times rinsed in deionized water. The vacuum evaporator was evacuated to a base pressure of about 2×10^{-6} mbar prior to deposition. Before deposition of the metallic contacts the wafers were outgassed at 900 °C, and during the deposition they were held at 180 °C. The deposition temperature was chosen in order to get better adhesion of the layers. Moreover, during the preparation of transparent TEM samples we anneal the embedded samples at 180 °C. Four different metal structures were prepared: Al (60 nm), Au (120 nm), Ti (50 nm)/Al (160 nm) and Ti (25 nm)/Au (115 nm). For the two latter cases the Ti layer was evaporated first directly on the substrate. The contacts with different areas were formed by standard photolithography. Consecutive heat treatments were applied at 300, 400, 700, and 900 °C for 10 min in high vacuum. The removal of the heated metallic contact layers was carried out by chemical etching in order to make visible the morphology of the grains grown into the GaN crystal.

The structure and surface morphology of annealed contacts were studied in a Philips CM 20 transmission electron microscope (XTEM) operated at 200 kV, in a JEOL 3010 high resolution transmission electron microscope (HREM) and in a LEO 1540 XB field-emission scanning electron microscope (FESEM), respectively. Energy dispersive X-ray analysis (EDS) was carried out by a NORAN Voyager system in the XTEM to determine the composition of different phases. Selected area electron diffraction (SAED) patterns were used to identify the phases formed in the annealed contacts. X-ray diffraction (XRD) measurements were used to observe the formation of new phases using a Philips PW 1050 diffractometer. For electrical characterisation I – V measurements were performed with a Keithley 236 series Source Measure Unit on the as deposited layers and after each annealing step between a large (about 0.5 cm²) pad and small contacts with different areas in the range of 0.01–1 mm². The temperature dependence of the I – V characteristics was studied in the range of 80–320 K for single Al layer. The

Schottky barrier height was evaluated for the thermionic emission theory by using the effective Richardson constant value of $24.6 \text{ A cm}^{-2} \text{ K}^{-2}$ [9].

3. Results and discussion

3.1. Structure and morphology

Transmission electron microscope study of XTEM samples have shown that all of the as-deposited metal layers have textured polycrystalline microstructure with c -planes of the metal grains lying mostly parallel to the c -plane of GaN. The metal–semiconductor interface was sharp. The contacts showed a bi-layer structure in the case of as-deposited Ti/Au and Ti/Al samples, as shown in Fig. 1a for the Ti/Au contact.

As a general picture, annealing induced metal interdiffusion and alloying in the contact layers. The thickness of the metal layers decreased (except Ti in Ti/Au) after annealing due to the interdiffusion and formation of alloys. On the other hand, Au layers bowed up during high temperature annealing, as, e.g. it can be seen in Fig. 1b for the Ti/Au contact annealed at 900 °C. XTEM investigations of the Ti/Au contact show that, after annealing at 900 °C for 10 min in vacuum, much of Au layer disappeared from the surface and recrystallization of Au metallization took place (Fig. 1b).

The HREM investigations of the (115 nm) Au/Ti (25 nm)/n-GaN contacts show that, after annealing at 900 °C larger Au(111) grains developed at the interface of metal/GaN (Fig. 2). It is well visible, that TiN and AuTi₃ phases arose at the vicinity of Ti/n-GaN interface.

The thermal diffusivity of Au in GaN is much higher than that of Ti. Our analysis revealed that Au diffused into the n-GaN layer (see Fig. 3). The composition of different phases of the

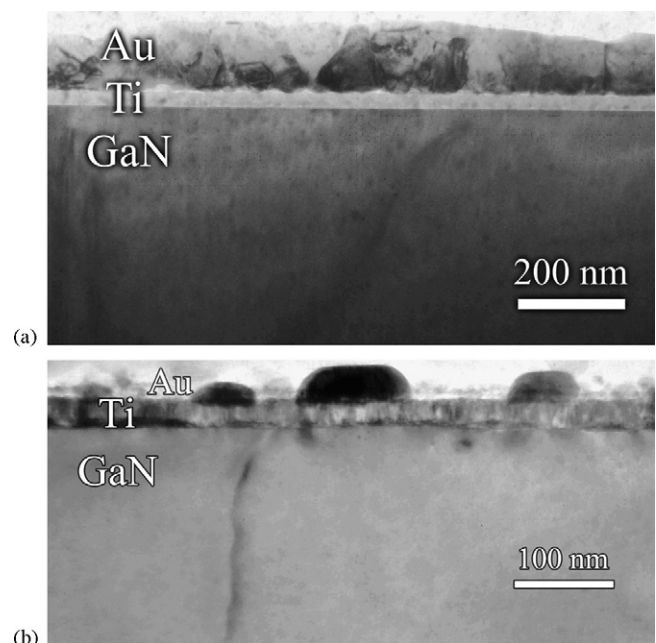


Fig. 1. Cross-sectional transmission electron microscope images of the Au/Ti/n-GaN contact (a) as-deposited (b) annealed at 900 °C.

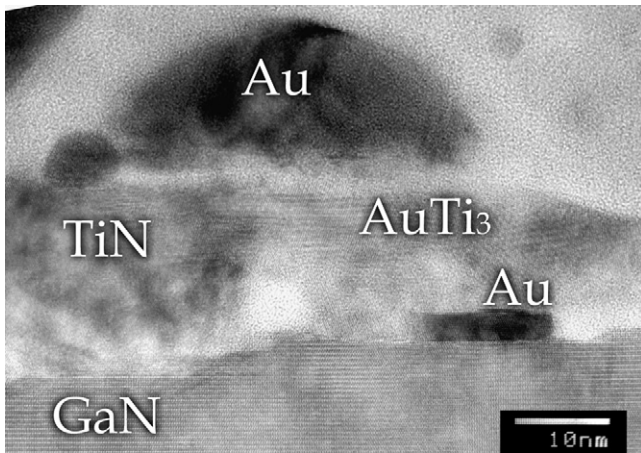


Fig. 2. HREM micrograph of the (115 nm) Au/Ti (25 nm)/n-GaN contact annealed at 900 °C.

interface of the Ti/Au layers by EDS annealed under these conditions is shown in Fig. 3b. EDS analysis confirms the presence of a Ga-rich phase containing also a significant amount of Au and Ti in the black pockets (Fig. 3a). The Ti content of EDS spectrum suggests the presence of a Ti-based nitride phase, which agrees with XRD indications of Ti_2N . The Au content revealed by our EDS analysis was found highest near the interface – in the black pocket (Fig. 3a) – but not penetrated significantly into the GaN (Fig. 3a).

The appearance of Au in the interfacial region clearly does not prevent good contact formation, and may be beneficial. The presence of the Au-containing phase may induce low Schottky barrier height (see Table 1).

A plan view TEM image in Fig. 4a shows dark grains indicating Au containing crystals in the 900 °C annealed GaN semiconductor. These grains grown into the GaN could be made visible after the removal of the metallic contact layers by chemical etching. EDS analysis of these crystallites indicate the presence of both Au and Ti (Fig. 4b).

The Au layer did not exhibit remarkable change after heat treatment at 700 °C, but it bowled up after heat treatment at 900 °C. However, there was a lateral diffusion of Au along the surface of Ti layer and GaN substrate at temperatures as low as 400 °C. A FESEM image of such a structure is presented in Fig. 5a. It can be seen that Au grains are present in the gap between the deposited metal electrodes. In the case of Ti/Au structure the Au layer began to bowl up at the edges of metal electrodes at 700 °C, as shown in Fig. 5b. During annealing at

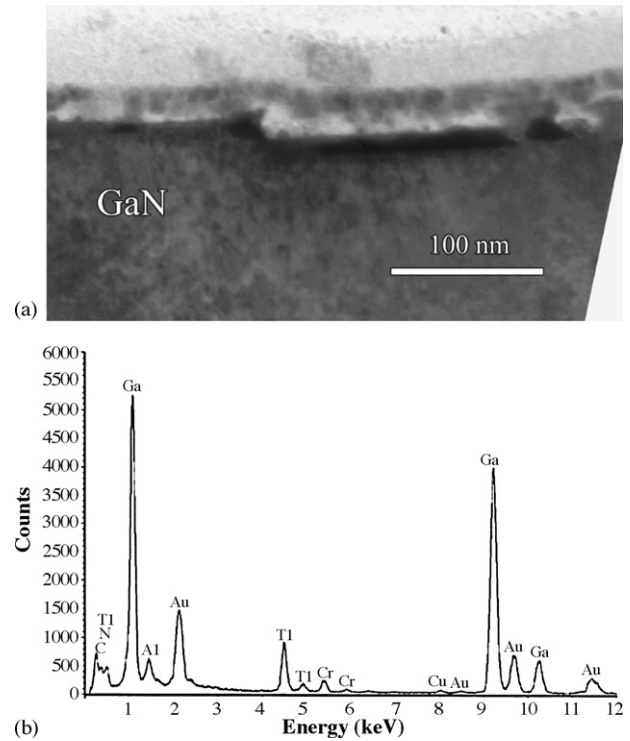


Fig. 3. (a) XTEM micrograph of the black pocket of n-GaN/Ti (25 nm)/Au (115 nm) contact annealed at 900 °C. (b) EDS spectrum of the black pocket and its surrounding of n-GaN/Ti (25 nm)/Au (115 nm) contact heated at 900 °C.

900 °C continuous films of upper Au film break up into discontinuous islands upon high-temperature annealing revealed by FESEM (Fig. 5c). The Ti layer remained continuous after this treatment as well.

The surfaces of Au and Ti/Au contacts (Fig. 5c) annealed at 900 °C have shown fractal-like structures since the surface patterns of these contacts showed apparent self-similarity [10]. The fractal dimension depends on the semiconductor materials and its technology, on choice of metal layers and on the conditions of heating, too. Island formation upon annealing of thin metal films on GaN is explained with the difference of surfaces energies between thin metal films and GaN that causes dewetting.

The Al layer began to become thin during the heat treatment at 700 °C. There was a lateral diffusion of Al as well during the heat treatment performed at this temperature. In the case of Ti/Au contacts, the continuity of the Ti layer was broken during the

Table 1

The room temperature current–voltage behaviour and the estimated Schottky barrier height as a function of annealing temperature

Annealing temperature (°C)	Contact metal			
	Al	Ti/Al	Au	Ti/Au
As-deposited	Linear ^a , $\phi_b < 0.35$ eV	Linear ^a , $\phi_b = 0.38$ eV	Rectifying, $\phi_b = 1.07$ eV	Rectifying, $\phi_b = 0.49$ eV
300	Linear ^a , $\phi_b < 0.35$ eV	Linear ^a , $\phi_b < 0.35$ eV	Rectifying, $\phi_b = 0.93$ eV	Rectifying, $\phi_b = 0.50$ eV
400	Linear ^a , $\phi_b < 0.35$ eV	Linear ^a , $\phi_b < 0.35$ eV	Rectifying, $\phi_b = 0.66$ eV	Rectifying, $\phi_b = 0.44$ eV
700	Rectifying, $\phi_b = 0.42$ eV	Linear ^a , $\phi_b < 0.35$ eV	Rectifying, $\phi_b = 0.56$ eV	Rectifying, $\phi_b = 0.43$ eV
900	Degraded	Degraded	Degraded	Linear ^a , $\phi_b < 0.36$ eV

^a Up to a current density level of 2 A mm^{-2} .

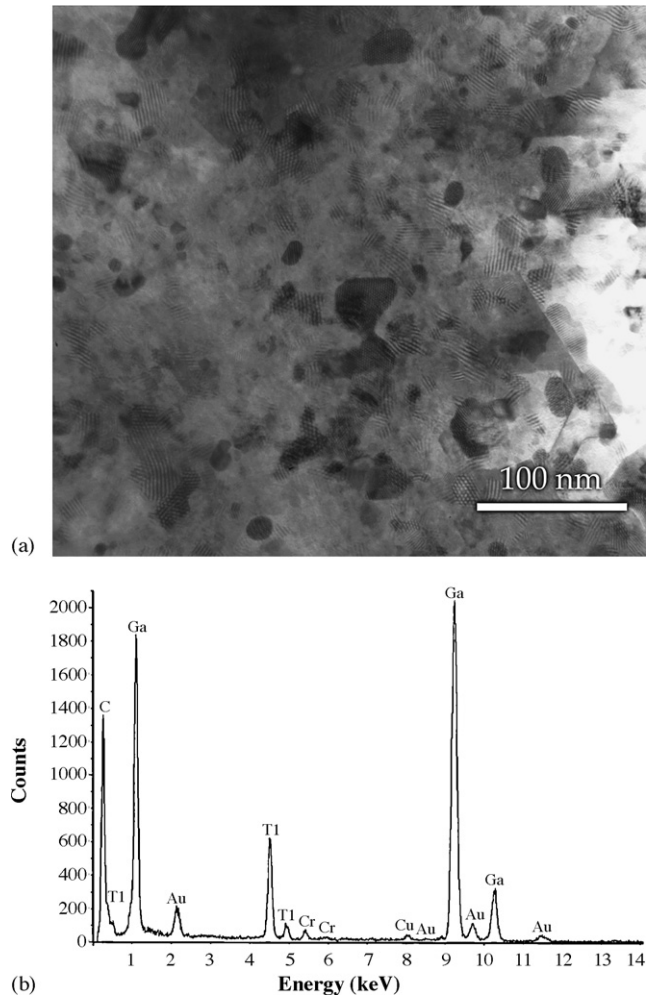


Fig. 4. (a) Plan view image of 900 °C annealed n-GaN/Ti (25 nm)/Au (115 nm) sample after removal of unreacted metallic layers. (b) EDS analysis of a dark grain on the plan view specimen.

annealing at 700 °C, Ti (or its alloys) islands were seen in the XTEM images. There was a lateral diffusion of either of the metals during the heat treatment at 900 °C, as observed in FESEM images (not shown).

3.2. XRD analysis

Fig. 6 shows XRD profiles of the Ti/Au and Ti/Al contacts after annealing at 700 and 900 °C. The separate layers of Au, Al and Ti on GaN can be seen in the profiles of the as-deposited samples (not shown). While no significant interdiffusion was detected by XRD between the Ti and Au in the as-deposited sample, the formation of Al–Ti alloys [$\text{Al}_2\text{Ti}(3\ 1\ 1)$, $\text{Al}_2\text{Ti}(0\ 0\ 2)$, $\text{Al}_3\text{Ti}(0\ 0\ 2)$ peaks] were observed even before thermal annealing. The annealing leads to metal interdiffusion and alloying in both bilayer metallization systems. The Ti/Al contact shows similar interaction between the Al and Ti layers at 400 °C, as deduced from the XRD data of as-deposited sample (not shown). XRD intensity profile of Ti/Al sample annealed at 700 °C (curve a in Fig. 6) shows further intermixing of Ti and Al layers [$\text{Al}_5\text{Ti}_3(3\ 2\ 0)$ at 28.6°, $\text{Al}_2\text{Ti}(3\ 1\ 1)$ at 38.9°, $\text{Al}_3\text{Ti}(1\ 0\ 3)$ at 39.15°]. A new Ti–N interface phase [$\text{Ti}_2\text{N}(1\ 1\ 1)$] – at the

39.3° 2θ position – formed in Ti/Al contact at 700 °C (curve a in Fig. 6). XRD suggest the possible presence of both Ti- rich and Al-rich interface phases after annealing at 700 °C. The profile of the n-GaN/Ti/Al sample annealed at 900 °C (curve b in Fig. 6) clearly shows that Al has diffused through the Ti, reached the GaN surface and AlN interface phase [$\text{AlN}(2\ 0\ 0)$ at $2\theta = 44.8^\circ$] was formed besides the TiN interface phase [$\text{Ti}_2\text{N}(2\ 1\ 1)$ at 51.0°] too. Furthermore, presence of the $\text{Ti}_{3,3}\text{Al}$ phase (3 1 1) at 37.9° 2θ can be supposed.

The XRD results of the as-deposited n-GaN/Ti/Au samples and those annealed at 400 °C are not shown. In addition to the characteristic peaks of GaN and $\alpha\text{-Al}_2\text{O}_3$, only the Au(1 1 1) and Au(2 0 0) Bragg reflection peaks can be observed. Annealing at high-temperatures resulted in changes of the XRD spectra due to the formation of several intermetallic phases. Significant change in the spectrum after annealing at 700 °C (curve c in Fig. 6) is the appearance of the peak at the $2\theta = 45.9^\circ$ position, this can be interpreted, as $\text{Au}_2\text{Ga}(5\ 1\ 2)$. The appearance of the Au_2Ga phase shows that Au diffused to the n-GaN layer and reacted with GaN.

Curve d in Fig. 6 shows the XRD spectrum of the sample annealed at 900 °C. The new peak at $2\theta = 20.7^\circ$ can be identified as another, the (4 0 0) peak of the same Au_2Ga phase, the presence of which was supposed after annealing at 700 °C. This phase is supposed to be the same the grains of which were observed by TEM on the plan view images (Fig. 4a) of the same sample after 900 °C annealing. Another significant feature of the XRD spectra was the shift in the (1 1 1) peak of the Au films toward smaller d -spacings with increasing annealing temperature. This shift might be attributed to changes caused by alloying and/or annealing-induced stress resulting from differences in their thermal expansion coefficients. This indicates that the Au diffused into the GaN epilayer at the interface vicinity. Further significant feature of the XRD spectra was the appearance of the peaks at about $2\theta = 40.6^\circ$ and 40.8° . These can be attributed to the $\text{Ga}_3\text{Ti}_2(2\ 2\ 0)$ and the $\text{Ti}_2\text{N}(2\ 1\ 0)$ peaks, respectively [11] (curve d in Fig. 6). The Ti(1 0 2) peak at 53.1° became wider and higher suggesting that the Ti layer emerged to the surface between the Au islands formed during annealing. This was supported by XTEM and FESEM examinations. The decrease of the (2 0 0) Au peak in the annealed sample (at 900 °C) was probably due to the Au being consumed by the reaction with Ga. Other metallic phases should also exist at the vicinity of metal/n-GaN interface but these reaction phases might be too thin to be detected in our XRD system.

3.3. Electrical behaviour

The special geometry of contacts makes possible to evaluate or estimate the Schottky barrier height of the contacts in most cases. The current flows through two Schottky (or ohmic) contacts with different areas connected back to back, and through the GaN layer. If the Schottky barrier height is less than 0.3–0.4 eV (depending on the series resistance), the contact usually exhibits linear I – V characteristics at room temperature and at low current levels indicating ohmic behaviour [12]. An example is presented in Fig. 7 for as-deposited Al contacts with

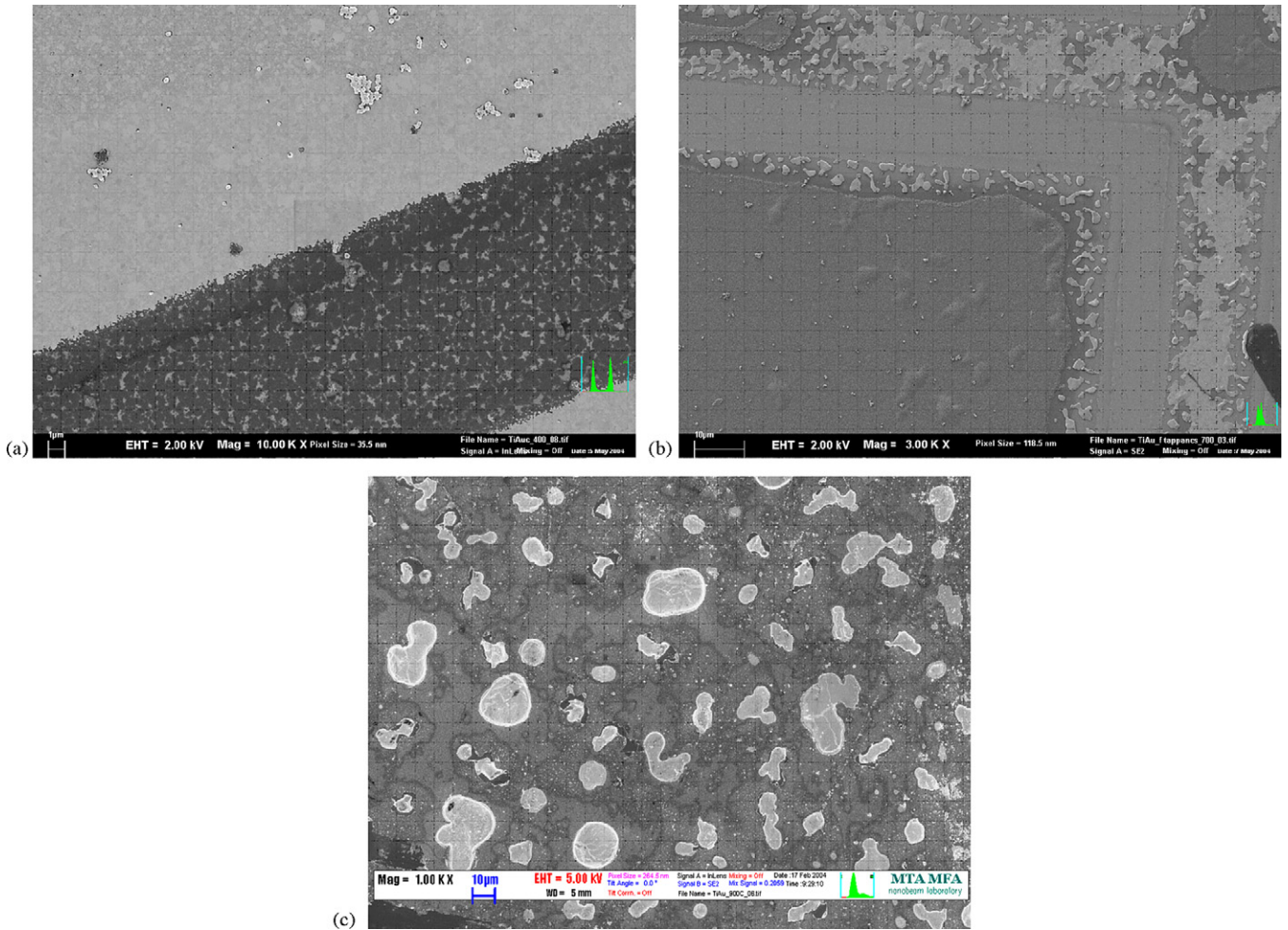


Fig. 5. Scanning electron microscope images of the Au/Ti/n-GaN contact (a) annealed at 400 °C, (b) annealed at 700 °C and (c) annealed at 900 °C.

an area of 1 mm². In this case the current is limited by the resistance of the GaN layer and of the spreading resistance of contact areas. However, decreasing the area of the smaller contact and the temperature, in many cases such a situation can be reached when the current is limited mainly by the Schottky barrier of the smaller contact for both forward and reverse

directions, as presented in Fig. 7 for the as-deposited Al contact with an area of 0.04 mm². In this case rectifying current–voltage behaviour is obtained, and the evaluation of Schottky barrier height is possible. Another example is shown in Fig. 8, where the semilogarithmic *I*–*V* characteristics obtained at room temperatures on the Au/Ti/n-GaN junctions annealed at 300 °C, are presented for different junction areas. The *I*–*V* characteristics for the area of 1 mm² are rectifying, but they can be hardly evaluated, while the characteristics obtained for 0.01 mm² can be evaluated easily.

The character of the room temperature *I*–*V* characteristics and the evaluated Schottky barrier heights are summarized in Table 1. The error of the evaluated barrier height values is estimated as ±0.03 eV. The as-deposited Al and Ti/Al contacts were linear. Contrary, the Au and Ti/Au contacts were rectifying but with different Schottky barrier heights. Although the Ti layer was underneath in both cases, there was a difference of about 0.1 eV between barrier heights for Ti/Au and Ti/Al contacts. This indicates that the upper metal influences the metal/GaN interface, i.e. the upper metal had to diffuse in and/or through the Ti layer during deposition, what was experimentally observed by XRD. The highest barrier height of 1.07 eV was obtained for Au. This value is rather close to the Schottky limit of 1.00 eV, i.e. to the difference between the

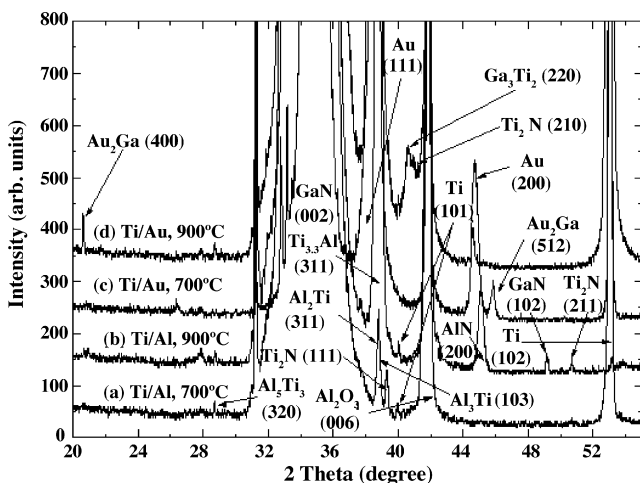


Fig. 6. XRD spectra of Ti/Al and Ti/Au contacts heat treated at 700 and 900 °C.

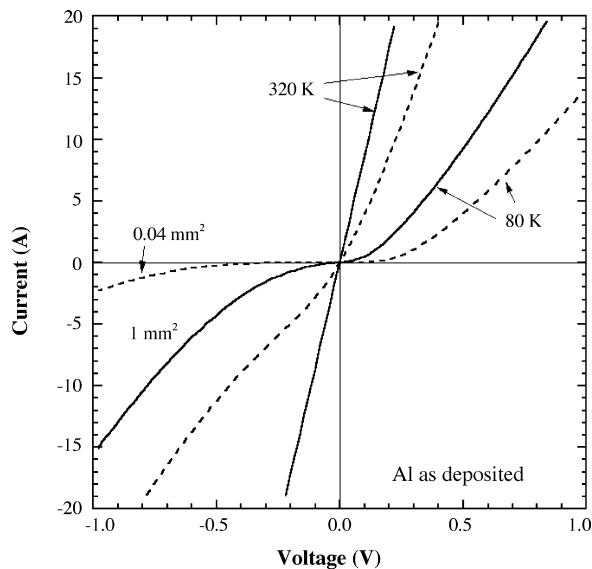


Fig. 7. Current–voltage characteristics of as deposited Al/n-GaN contacts with area of $200\ \mu\text{m} \times 200\ \mu\text{m}$ (dashed lines) and $1\ \text{mm} \times 1\ \text{mm}$ (solid lines) measured at 80 and 320 K.

metal work function and semiconductor electron affinity [13], which values are 5.10 eV for Au [14] and 4.10 eV for GaN [3], respectively. This indicates a low interface state density in the studied as-deposited Au contacts. While as-deposited Au and Ti/Au contacts exhibited nonlinear I – V characteristics, as-deposited Al and Ti/Al contacts had linear I – V characteristics. This latter must be due to the low Al work function of 4.08 eV, which yields a Schottky limit of about zero to GaN. As deposited Ti/Al contacts showed linear I – V characteristics with higher conductivity than Al contacts. Both Al and Ti/Al contacts exhibited linear I – V characteristics after annealing steps at 300 and 400 °C as well. Annealing decreased the obtained barrier height with the exception of Al contacts, which

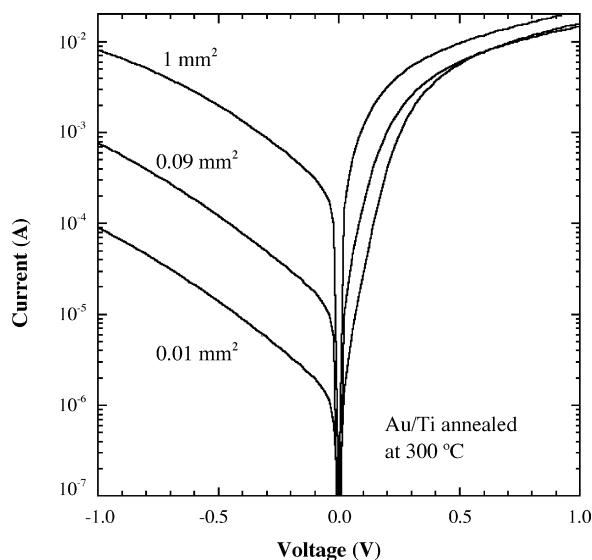


Fig. 8. Semilogarithmic current–voltage characteristics of Au/Ti/n-GaN contacts annealed at 300 °C with area of $100\ \mu\text{m} \times 100\ \mu\text{m}$, $300\ \mu\text{m} \times 300\ \mu\text{m}$, and $1\ \text{mm} \times 1\ \text{mm}$ measured at room temperature.

showed an increased barrier height after annealing at 700 °C. After annealing at 900 °C most of the contacts degraded, only the Ti/Au contacts were preserved good enough to be measured, but their I – V characteristics became linear.

Comparing the values of electrical measurements after various heat treatments suggests that the presence of the Al-containing phase in contact with the interface causes a decrease in Schottky barrier height ($\phi_b < 0.36\ \text{eV}$, Table 1).

4. Conclusions

Metallic contacts on n-GaN annealed up to 900 °C have been studied by XTEM, HREM, FESEM, XRD and I – V characteristics using the combinations of Al, Au and Ti. The structure of the as-deposited metal layers was found textured polycrystalline. Annealing yielded interdiffusion, lateral diffusion, alloying and bowling up of the Au layers.

XRD studies revealed that obtaining low Schottky barrier requires the penetration of Al and Au through the Ti layer to reach the GaN surface in addition to N out-diffusing from the GaN surface and into the metal layers. New Ti_2N , Au_2Ga and Ga_3Ti_2 interface phases formed in Ti/Au contact at 900 °C, new Ti_2N phase formed in Ti/Al contact at 700 and 900 °C, as well as new AlN interface phase developed in Ti/Al contact at 900 °C.

The FESEM investigations indicated the effect of increasing the surface roughness – except Ti/Al – after annealing. Au diffusion into the n-GaN were revealed by XTEM, EDS, HREM and XRD.

High-temperature thermal treatment degraded most contacts. Due to Au diffused into the n-GaN layer at 900 °C, Ti/Au contact did not degraded, but became linear. The presence of gold at the interface might be a potential problem in high power devices, but the presence of gold containing grains without degradation of the present contacts is promising. The dependence of the Schottky barrier heights on the annealing temperature may be attributed to changes of surface morphology of metal films on the n-GaN surface and variation of crystal defects at the interface vicinity.

Acknowledgements

The authors are grateful to Á. Barna for his ideas and discussion on the experiments.

This work has been supported in part by the (Hungarian) National Scientific Research Fund (OTKA) under Grants Nos. T047141, T048696, and M041689. One of the authors (B.P.) thanks the support of the Bolyai Janos Scholarship (Hungary).

References

- [1] Z.-F. Fan, S.N. Mohammad, W. Kim, O. Aktas, A.E. Botchkarev, H. Morkoç, Appl. Phys. Lett. 68 (1996) 1672.
- [2] S. Ruvimov, Z. Liliental-Weber, J. Washburn, K.J. Duxstad, E.E. Haller, Z.-F. Fan, S.N. Mohammad, W. Kim, A.E. Botchkarev, H. Morkoç, Appl. Phys. Lett. 69 (1996) 1556.
- [3] J.S. Foresi, T.D. Moustakas, Appl. Phys. Lett. 62 (1993) 2859.
- [4] B.P. Luther, S.E. Mohny, T.N. Jackson, M. Asif Khan, Q. Chen, J.W. Yang, Appl. Phys. Lett. 70 (1997) 57.

- [5] S. Ruvimov, Z. Liliental-Weber, J. Washburn, D. Qiao, S.S. Lau, Paul K. Chu, *Appl. Phys. Lett.* 73 (1998) 2582.
- [6] N.A. Papanicolaou, K. Zekentes, *Solid State Electron.* 46 (2002) 1975.
- [7] A. Motayed, R. Bathe, M.C. Wood, O.S. Diouf, R.D. Vispute, S. Noor Mohammad, *J. Appl. Phys.* 93 (2003) 1087.
- [8] E. Frayssinet, B. Beaumont, J.P. Faurie, P. Gibart, Zs. Makkai, B. Pécz, P. Lefebvre, P. Valvin, *MRS Internet J. Nitride Semicond. Res.* 7 (2002) 8.
- [9] Y. Liu, M.Z. Kauser, M.I. Nathan, P.P. Ruden, S. Dogan, H. Morkoç, *Appl. Phys. Lett.* 84 (2004) 2112.
- [10] T. Vicsek, *Fractal Growth Phenomena*, World Scientific, Singapore, 1989 .
- [11] S.E. Lofland, J.D. Hettinger, K. Harrell, P. Finkel, S. Gupta, M.W. Barsoum, G. Hug, *Appl. Phys. Lett.* 84 (2004) 508.
- [12] Zs.J. Horváth, M. Ádám, I. Szabó, M. Serényi, Vo. Van Tuyen, *Appl. Surf. Sci.* 190 (2002) 441.
- [13] S.M. Sze, *Physics of Semiconductor Devices*, 2nd ed., Wiley, New York, 1981, p. 247.
- [14] H.B. Michaelson, *IBM J. Res. Dev.* 22 (1978) 72.